

## Research papers

## Assessing the controls and uncertainties on mean transit times in contrasting headwater catchments

Ian Cartwright<sup>a,\*</sup>, Dylan Irvine<sup>a,b</sup>, Chad Burton<sup>a,c</sup>, Uwe Morgenstern<sup>d</sup><sup>a</sup> School of Earth, Atmosphere and Environment, Monash University, Clayton, Vic. 3800, Australia<sup>b</sup> School of the Environment, Flinders University, GPO Box 2100, SA 5001, Australia<sup>c</sup> School of Geography and the Environment, University of Oxford, South Parks Road, Oxford OX1 3QY, United Kingdom<sup>d</sup> GNS Science, Lower Hutt 5040, New Zealand

## ARTICLE INFO

## Article history:

Received 2 June 2017

Received in revised form 2 November 2017

Accepted 3 December 2017

Available online 6 December 2017

## Keywords:

Catchments

Rivers

Tritium

Transit times

Tritium

Australia

## ABSTRACT

Estimating the time required for water to travel through headwater catchments from where it recharges to where it discharges into streams (the transit time) is important for understanding catchment behaviour. This study uses tritium ( $^3\text{H}$ ) activities of stream water to estimate the mean transit times of water in the upper Latrobe and Yarra catchments, southeast Australia, at different flow conditions. The  $^3\text{H}$  activities of the stream water were between 1.26 and 1.99 TU, which are lower than those of local rainfall (2.6 to 3.0 TU).  $^3\text{H}$  activities in individual subcatchments are almost invariably lowest at low streamflows. Mean transit times calculated from the  $^3\text{H}$  activities using a range of lumped parameter models are between 7 and 62 years and are longest during low streamflows. Uncertainties in the estimated mean transit times result from uncertainties in the geometry of the flow systems, uncertainties in the  $^3\text{H}$  input, and macroscopic mixing. In addition, simulation of  $^3\text{H}$  activities in FEFLOW indicates that heterogeneous hydraulic conductivities increase the range of mean transit times corresponding to a specific  $^3\text{H}$  activity. The absolute uncertainties in the mean transit times may be up to  $\pm 30$  years. However, differences between mean transit times at different streamflows in the same catchment or between different subcatchments in the same area are more reliably estimated. Despite the uncertainties, the conclusions that the mean transit times are years to decades and decrease with increasing streamflow are robust. The seasonal variation in major ion geochemistry and  $^3\text{H}$  activities indicate that the higher general streamflows in winter are sustained by water displaced from shallower younger stores (e.g., soils or regolith). Poor correlations between  $^3\text{H}$  activities and catchment area, drainage density, mean slope, distance to stream, and landuse, imply that mean transit times are controlled by a variety of factors including the hydraulic properties of the soils and aquifers that are difficult to characterise spatially. The long mean transit times imply that there are long-lived stores of water in these catchments that may sustain streamflow over drought periods. Additionally, there may be considerable delay in contaminants reaching the stream.

© 2017 Elsevier B.V. All rights reserved.

## 1. Introduction

Documenting the time that groundwater takes to flow through a catchment from the recharge area to where it discharges into the stream (the transit time) is important for understanding catchment behaviour (McGuire and McDonnell, 2006; Hrachowitz et al., 2009a,b; Soulsby et al., 2009; McDonnell et al., 2010; Stewart et al., 2010, 2012; Duvert et al., 2016). For example, catchments with long transit times contain long-lived stores of water that may sustain streamflow during droughts (Morgenstern et al., 2010; Cartwright and Morgenstern, 2015). In addition, the mean

transit time governs the time required for contaminated groundwater to reach the stream (Böhlke and Michel, 2009; Stewart et al., 2011; Morgenstern et al., 2015; Soulsby et al., 2015).

Due to high rainfall totals that commonly significantly exceed evapotranspiration rates and high runoff rates on indurated or crystalline rocks, catchment headwaters may contribute a significant proportion of the total streamflow for many river systems. Headwater streams can provide much of the water that is eventually used downstream for human consumption, recreation, agriculture, and/or industry (Freeman et al., 2007). While some headwater catchments retain native vegetation, many now consist of plantation forests, pastures, crops, and/or urban developments. The impact of such developments on headwater catchments is not always well understood. Replacement of native eucalypt

\* Corresponding author.

E-mail address: [ian.cartwright@monash.edu](mailto:ian.cartwright@monash.edu) (I. Cartwright).

vegetation with crops and grasses over the last 200 years in south-east Australia had a profound impact on both groundwater and surface water systems (Allison et al., 1990). The high transpiration rates of the native vegetation led to low groundwater recharge rates resulting in deep water tables. Recharge rates following land clearing are significantly higher (Allison et al., 1990; Cartwright et al., 2007), which has caused the water table to rise and resulted in some former ephemeral streams becoming perennial.

Lowland rivers are commonly hosted by sediments that contain large stores of groundwater that may make significant contributions to streamflow especially during low flow periods (Winter, 1999; Tetzlaff and Soulsby, 2008; Cartwright et al., 2011, 2014; Duvert et al., 2016). By contrast, headwater streams may occur on indurated or crystalline rocks that have limited groundwater systems. The observation that many headwater streams are perennial and flow over prolonged dry periods indicates, however, that they receive water from the soils, regolith, or fractures (Rice and Hornberger, 1998; Soulsby et al., 2005; Hrachowitz et al., 2009a; Cartwright and Morgenstern, 2015). The locations and transit times of these water stores are commonly not well understood, which hampers our understanding and management of headwater catchments.

### 1.1. Determining mean transit times

Water flowing through catchments follows flow paths of varying length, and the water discharging into streams has a range of transit times governed by the geometry of the flow paths. Lumped parameter models, which describe the distribution of water with different residence times in homogeneous aquifers with simplified geometries and uniform recharge rates, are commonly used to estimate mean transit times of water sampled from aquifers or streams (Maloszewski and Zuber, 1982; Cook and Bohlke, 2000; Maloszewski, 2000; McGuire and McDonnell, 2006; Leray et al., 2016). The radioactive isotope tritium ( $^3\text{H}$ ) with a half-life of 12.32 years may be used to estimate transit times where these are years to decades (Morgenstern et al., 2010).  $^3\text{H}$  is part of the water molecule and geochemical or biogeochemical reactions in the soils or aquifers do not affect its abundance. Consequently, the calculated transit times reflect water flow through both the unsaturated zone and within the aquifer.

Rainfall  $^3\text{H}$  activities peaked in the 1950 s to 1960 s due to the production of  $^3\text{H}$  in atmospheric thermonuclear tests (the  $^3\text{H}$  “bomb pulse”). The  $^3\text{H}$  activities of the remnant bomb pulse waters in the southern hemisphere have now largely decayed below those of modern rainfall, which permits mean transit times to be estimated from individual  $^3\text{H}$  activities (Morgenstern et al., 2010). However, this approach requires that the lumped parameter models be assigned based on the known or assumed geometry of the flow system. Groundwater with high bomb pulse  $^3\text{H}$  activities is still present in the northern hemisphere and mean transit times may be estimated from lumped parameter models using time-series of  $^3\text{H}$  activities (Maloszewski and Zuber, 1982; Blavoux et al., 2013; Morgenstern et al., 2015). While this increases the duration of the studies, it does allow an assessment of the suitability of the lumped parameter model. The reduction of bomb pulse  $^3\text{H}$  activities in the southern hemisphere make it impracticable to constrain lumped parameter models using future time-series measurements (Cartwright and Morgenstern, 2016b).

While not being able to assess the form of the lumped parameter model introduces uncertainty, the calculated mean transit times are far less sensitive to the choice of lumped parameter model than is the case for northern hemisphere catchments. Additionally this approach allows the changing mean transit times at different flow conditions to be estimated (Morgenstern et al.,

2010; Duvert et al., 2016; Cartwright and Morgenstern, 2015, 2016b). Further, because the  $^3\text{H}$  activities of the remnant bomb pulse waters are below those of modern rainfall, water with low  $^3\text{H}$  activities has longer mean transit times than water with high  $^3\text{H}$  activities, permitting a robust assessment of relative mean transit times.

The pathways of groundwater inflows to a stream are potentially more complex than assumed in the lumped parameter models. The aggregation of water from different flow systems potentially produces water samples with residence time distributions that do not correspond to those in the lumped parameter models. Mean transit times calculated from the aggregated waters are generally lower than the actual mean transit times (Suckow, 2014; Kirchner, 2016; Stewart et al., 2017). Lumped parameter models also assume that the aquifers are homogeneous. However, hydraulic conductivities are heterogeneous at a variety of scales due to weathering, the presence of fractures, and lithological variations. Similar to aggregation, heterogeneities in hydraulic conductivity result in macroscopic dispersion that also may result in different  $^3\text{H}$  vs. mean transit time relationships to those predicted by simple flow models (Weissmann et al., 2002; McCallum et al., 2014, McCallum et al., 2015).

### 1.2. Controls on mean transit times

Identifying the controls on mean transit times is important for understanding catchment behaviour and for making first order predictions of mean transit times in unstudied catchments. Mean transit times are a function of recharge rates, groundwater flow velocities, and flow path lengths. In southeast Australia, cleared catchments may have lower evapotranspiration and higher recharge rates and thus shorter mean transit times than those that retain native vegetation (Allison et al., 1990; Cartwright et al., 2007). The hydraulic conductivity of the aquifers, which in basement rocks is controlled by the degree of weathering and interconnectivity and transmissivity of fractures (Lachassagne et al., 2011), also influences mean transit times. The mobilisation of stores of water with different residence times (e.g., soil waters, water from the regolith, or water in perched aquifer systems) as the catchment wets up following rainfall also controls net mean transit times (Hrachowitz et al., 2009a, 2013).

Catchment geomorphology and geometry influences the length of the flow paths and hydraulic gradients (e.g., McGuire et al., 2005; McGuire and McDonnell, 2006; Hrachowitz et al., 2009b, 2010; Soulsby et al., 2009). Large catchments may have some long groundwater flow paths with long transit times. Catchments with higher drainage densities may contain numerous short groundwater flow paths and consequently have shorter mean transit times. Steeper catchments have higher hydraulic gradients that may lead to more rapid groundwater flow and shorter mean transit times.

There may be correlations between  $^3\text{H}$  activities and major ion concentrations or ratios that allow first order estimates of mean transit times to be made (Morgenstern et al., 2010; Cartwright and Morgenstern, 2015, 2016a, 2016b; Duvert et al., 2016; Beyer et al., 2016). These correlations commonly stem from mineral dissolution reactions progressing further in older waters. Evapotranspiration also increases major ion concentrations, especially in semi-arid areas, and catchments with high evapotranspiration rates are likely to have lower recharge rates and longer mean transit times. Catchments with high evapotranspiration rates are also likely to have lower runoff coefficients (the percentage of rainfall that is exported annually by the stream), and runoff coefficients may be a proxy for mean transit times (Cartwright and Morgenstern, 2015).

### 1.3. Objectives

This paper estimates mean transit times at different stream-flows in headwater streams from the Latrobe and Yarra catchments in southeast Australia using  $^3\text{H}$  activities of stream water. Additionally, it assesses whether catchment attributes, such as drainage density, catchment area, landuse, or slope, control mean transit times. The two catchments differ markedly in the extent of land clearing and it was hypothesised that this would result in different mean transit times. Further, it explores whether there are geochemical proxies for  $^3\text{H}$  that can provide first order estimates of mean transit times. In addition to assessing the uncertainties in mean transit times resulting from using different lumped parameter models, aggregation, uncertainties in the  $^3\text{H}$  input function, it uses a numerical model to address the impact of heterogeneities in hydraulic conductivities on the estimated mean transit times. While it is based on a specific area, these themes are relevant to headwater catchments globally.

## 2. Study area

### 2.1. Upper Yarra catchment

The upper Yarra catchment drains the eastern slopes of the Dandenong Ranges in southeast Victoria. Annual rainfall across the catchment averages 750–1000 mm and average annual evapotranspiration rates are 500–600 mm (Bureau of Meteorology, 2017). Rainfall occurs throughout the year, but is highest in the winter months when evapotranspiration rates are lowest. This results in winter streamflows being higher than those in summer (Melbourne Water, 2017). The main streams are Woori Yallock Creek, Wandin Yallock Creek, and Stringybark Creek, all of which are perennial tributaries of the Yarra River (Fig. 1). Average streamflows are  $6.3 \times 10^7 \text{ m}^3 \text{ yr}^{-1}$  in Woori Yallock Creek  $1.84 \times 10^5 \text{ m}^3 \text{ yr}^{-1}$  in Wandin Yallock Creek, and  $3.7 \times 10^6 \text{ m}^3 \text{ yr}^{-1}$  in Stringybark Creek (Melbourne Water, 2014).

The upper Yarra catchment comprises a basement of indurated Silurian-Devonian turbidites and granitic rocks (including granites and extensive rhyolites). These rocks are overlain by thin Devonian calcareous sandstones and Tertiary basaltic volcanics (van den Berg, 1975; Energy and Earth Resources, 2017) (Fig. 1b). Thin deposits of recent alluvial sediments occur along some of the major streams. Weathering is variable across the catchment. The basaltic volcanics commonly occur on the ridges and are weathered to depths of up to 50 m with kaolinite and montmorillonite common weathering products (Shugg, 1996; Tweed et al., 2005). The turbidites and granites have weathered zones that are generally <5 m thick and which contain kaolinite and smectites as weathering products.

Groundwater flow is hosted in fractures and the weathered zones of the indurated rocks and in the more permeable zones of the basalts (Shugg, 1996; Tweed et al., 2005). Horizontal hydraulic conductivities in the unweathered basalts are  $\sim 0.3 \text{ m day}^{-1}$  (Shugg, 1996) but, based on the distribution of groundwater residence times, hydraulic conductivities in the weathered zones are locally  $>1 \text{ m day}^{-1}$  (Tweed et al., 2005). The metasediments and granites in nearby areas have hydraulic conductivities of  $0.001\text{--}1 \text{ m day}^{-1}$ , with the higher hydraulic conductivities occurring in weathered zones close to the land surface and zones of more intense fracturing (van den Berg and Morand, 1997). The hydraulic conductivity of the alluvial sediments are typically  $0.2\text{--}5 \text{ m day}^{-1}$ . Groundwater recharges on the ridges and discharges into the lower reaches of many of the rivers (Tweed et al., 2005).

Approximately 84% of this part of the upper Yarra catchment has been cleared. Current landuse includes dairying, horticulture,

vineyards, and grazing and a significant amount of low-density urban developments (Melbourne Water, 2014). There is an annual water allocation of  $9.5 \times 10^6 \text{ m}^3$  from Woori Yallock Creek (approximately 15% of annual streamflow), although <30% of this allocation is typically used (Melbourne Water, 2014).

### 2.2. Upper Latrobe catchment

The headwaters of the Latrobe catchment drain the southern slopes of the Yarra Ranges (Fig. 1). The upper Latrobe catchment has an average annual rainfall of between 1100 and 1400 mm, and average annual evapotranspiration rates are 500–600 mm (Bureau of Meteorology, 2017). The upper Latrobe River is perennial and the upper catchment includes the Loch and Tooronga Rivers that join the Latrobe River near Noojee. The total catchment area upstream of the lowermost sampling site at Willow Grove is  $559 \text{ km}^2$  and the long-term average streamflow of the Latrobe River at Willow Grove is  $10^8 \text{ m}^3 \text{ yr}^{-1}$  (Department of Environment Land Water and Planning, 2017). As with the Yarra catchment, streamflows in the upper Latrobe catchment are higher in winter (e.g., Fig. 2).

Granites, granodiorites, and metamorphosed Silurian-Devonian turbidites, which again host groundwater flow mainly in weathered zones and fractures, dominate the north of the upper Latrobe catchment (Fig. 1b). The south of the catchment also includes coarse-grained Pliocene sands and gravels, minor granites, and basaltic volcanics (van den Berg, 1975; Energy and Earth Resources, 2017). Thin deposits of recent alluvial sediments occur along the major streams. Relatively little is known about groundwater flow in this catchment. However, given the similarities in lithologies, the hydraulic conductivities are likely to be similar to those in the upper Yarra catchment. Weathering is deepest on the ridges and the metasediments and granites commonly have weathering zones that are a few metres thick (van den Berg, 1975). Groundwater recharges on the ridges and discharges into the Latrobe River (Southern Rural Water, 2014).

By contrast with the upper Yarra catchment, the upper Latrobe catchment is dominated by native eucalypt forest, much of it in the Alpine National Park. Additionally, there are plantation forests, mainly along the Loch Valley and zones of mixed agriculture (including dairying, vineyards, and grazing) around Noojee and Willow Grove. There is minimal groundwater use in the upper Latrobe catchment (Southern Rural Water, 2014).

## 3. Methods

### 3.1. Sampling and analytical techniques

A one year aggregated rainfall sample was collected from a rainfall collector located at Yarra Junction, which is close to the boundary between the two catchments (Fig. 1a). Four rounds of stream samples were collected at varying flow conditions (Table A1, Fig. 2) from six sites in the upper Latrobe catchment with areas ranging from 62 to  $559 \text{ km}^2$  and four sites in the upper Yarra catchment with areas ranging from 9 to  $325 \text{ km}^2$  (Fig. 1). Sampling avoided the high streamflows that occur immediately following rainfall in order to characterise the average seasonal flows (Fig. 2). April 2015 and March 2016 represent low flow conditions at the end of the austral summer, August 2015 represents high winter flows, and November 2015 represents intermediate spring flows. Sub-daily streamflows are measured at the Willow Grove, Noojee, Lower Loch, and Gentle Annie sites in the upper Latrobe catchment and the Stringybark, Woori Yallock, Wandin Yallock, and Cockatoo sites in the upper Yarra catchment (Department of

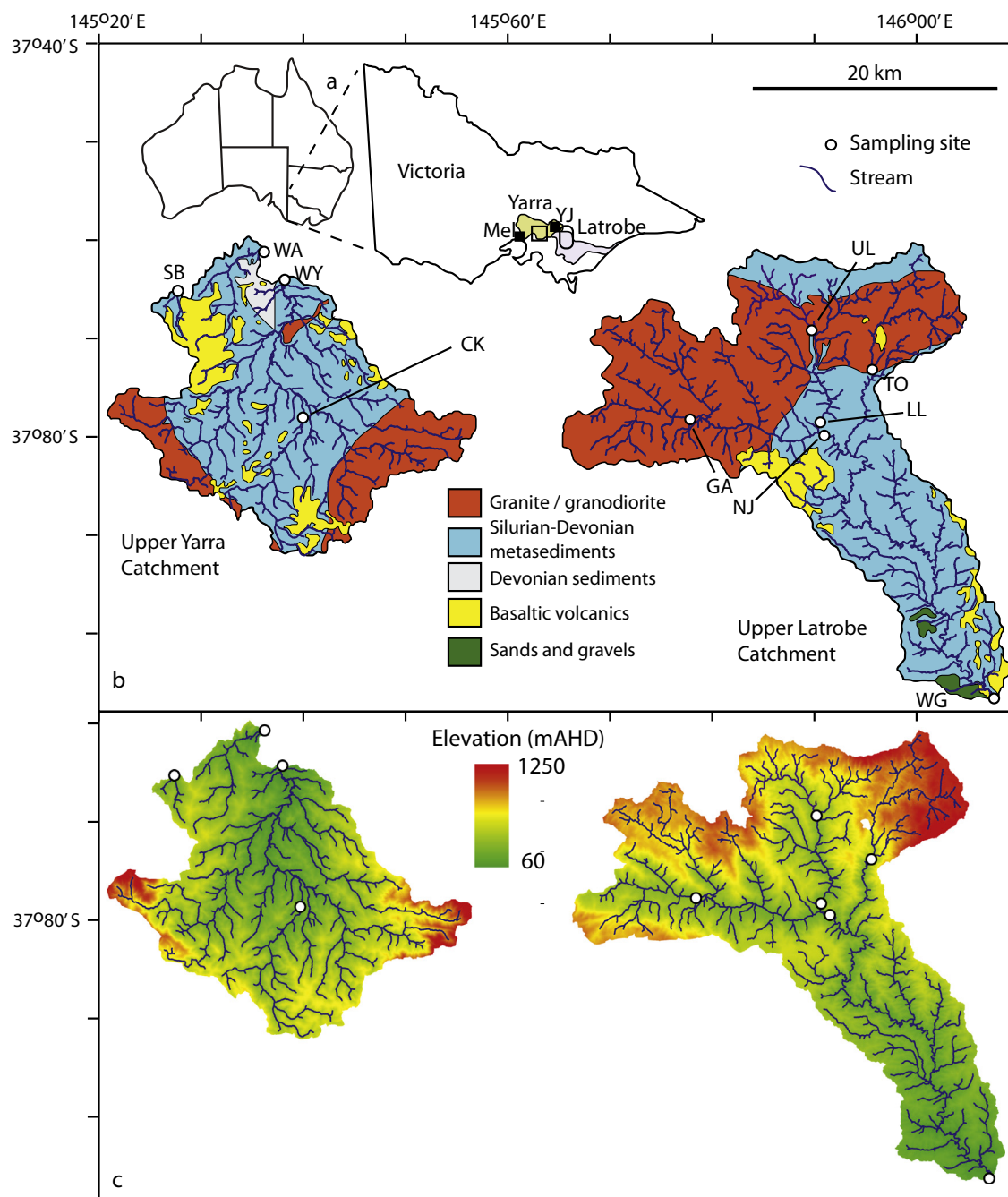


**Fig. 1.** (a). General location map of the study area, boxes show locations of the upper Yarra and Latrobe catchments. Abbreviations Mel = Melbourne, YJ = Yarra Junction. (b). General geology map of the upper Latrobe and upper Yarra catchments (Energy and Earth Resources, 2017) together with the stream network. Sampling sites: GA = Gentle Annie; LL = Lower Lock; NJ = Noojee; TO = Toorong; UL = Upper Loch; WG = Willowgrove; CK = Cockatoo; SB = Stringybark; WA = Wandin Yallock; WY = Woori Yallock. The coordinates of the sampling sites are in Table A1. 1b. Digital elevation maps of the upper Latrobe and upper Yarra catchments (Victoria Open Data, 2016).

Environment Land Water and Planning, 2017; Melbourne Water, 2017).

Electrical conductivity (EC) was measured in the field using a calibrated TPS meter and electrodes. Cation concentrations were measured at Monash University using a Thermo Fischer ICP-OES on samples that had been filtered through 0.45  $\mu\text{m}$  cellulose nitrate filters and acidified to  $\text{pH} < 2$  using double-distilled 16 M  $\text{HNO}_3$ . Anion concentrations were measured at Monash University on filtered unacidified samples using a Thermo Fischer ion chromatograph. Geochemical data is presented in Table A1 in Supplement 1. The precision of anion and cation analyses based

on replicate analyses is  $\pm 2\%$  and the accuracy based on analysis of certified water standards is  $\pm 5\%$ .

$^3\text{H}$  activities were measured at GNS following Morgenstern and Taylor (2009). Following vacuum distillation and electrolytic enrichment,  $^3\text{H}$  activities were determined using liquid scintillation in Quantulus ultra-low-level counters. Tritium enrichment was by a factor of 95, which yields a detection limit of 0.02 TU. Deuterium calibration of each sample ensures reproducibility of tritium enrichment of 1%.  $^3\text{H}$  activities are expressed in tritium units (TU) where 1 TU represents a  $^3\text{H}/^1\text{H}$  ratio of  $1 \times 10^{-18}$ . Relative precision ( $1\sigma$ ) of individual analyses are 1.5–2.5% (Table A1).



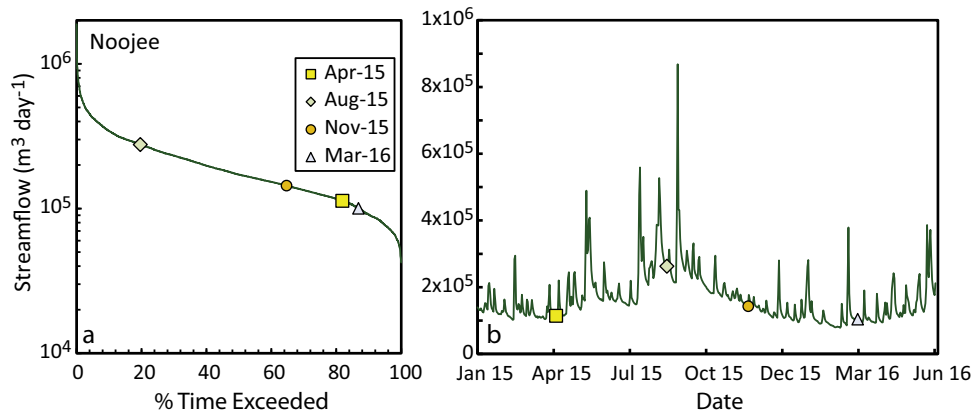


**Fig. 2.** (a). Sampling times for this study relative to the flow frequency curve for Noojee (Fig. 1). (b). Variation in streamflows at Noojee between January 2015 and June 2016. Data from Department of Environment Land Water and Planning (2017).

### 3.2. Catchment attributes

Catchment attributes were estimated using ArcGIS 10 (ESRI®) and datasets from Victoria Open Data (2016). The Hydrology Modelling tools were used to generate the stream network from a 10 m digital elevation model (Fig. 1c). A threshold catchment area of 50 Ha reproduces the observed perennial stream network of the area. Subcatchment areas upstream of each sampling site were calculated using the watershed tool, and drainage densities calculated as the total stream length in each subcatchment divided by the subcatchment area. Mean slopes and the mean and maximum distance to the stream were calculated using the Spatial Analysis tools. Vector-based landuse datasets were converted to raster formats and reclassified. Landuse was assigned as forest (includes native vegetation and some plantations) and cleared land, which includes urban and mixed agricultural regions (pasture, horticulture, and crops).

### 3.3. Mean transit times

Mean transit times were calculated using the exponential, exponential-piston flow, and dispersion lumped parameter models implemented in the TracerLPM Excel workbook (Jurgens et al., 2012) as described in Supplement 2. For the exponential-piston flow models, EPM ratios of 0.33 (75% exponential flow and 25% piston flow) and 1 (50% exponential flow and 50% piston flow) were used. This model accords with the expected geometry of flow in the catchment (vertical recharge through the unsaturated zone followed by flow along flow paths of varying length). For the dispersion model, values of DP of 0.1 and 1 were used, which is the range generally adopted for kilometre-scale flow systems (Maloszewski, 2000). These lumped parameter models have successfully reproduced time-series  $^3\text{H}$  activities of stream water elsewhere (Maloszewski and Zuber, 1982; Blavoux et al., 2013; Morgenstern et al., 2015).

The annual average  $^3\text{H}$  activities of rainfall in Melbourne (Tadros et al., 2014; International Atomic Energy Agency, 2017) were used as the  $^3\text{H}$  input function. Rainfall  $^3\text{H}$  activities in Melbourne peaked at approximately 62 TU in 1965 and then declined exponentially to present-day values. The calculations initially adopted a present-day  $^3\text{H}$  activity of 2.8 TU based on the  $^3\text{H}$  activity of rainfall from Yarra Junction (Table A1) and the expected  $^3\text{H}$  activity of rainfall in this area (Tadros et al., 2014). A  $^3\text{H}$  activity of 2.8 TU was also used for rainfall from the years before the atmospheric nuclear tests. Mean transit times were calculated by matching the measured  $^3\text{H}$  activity in the stream water with that predicted from the lumped parameter model.

### 3.4. Numerical modelling

The lumped parameter models assume homogeneous aquifer properties that lead to a regular distribution of groundwater flow paths and mean transit times. However, most catchments have heterogeneous hydraulic conductivities (Weissmann et al., 2002; McCallum et al., 2014, McCallum et al., 2015). Two-dimensional numerical simulations were performed using FEFLOW (Diersch, 2013) as described in Supplement 2. The purpose of the modelling was not to simulate flow in these catchments but to explore the impact of heterogeneous hydraulic conductivities on mean transit times.

Briefly, the FEFLOW model domain was 10,000 m in the longitudinal (x) direction and 25 m in the vertical (z) direction (Fig. S1a). The hydraulic boundary conditions were a constant flux at the top to simulate  $50 \text{ mm yr}^{-1}$  recharge and a constant head at the model outlet (Fig. S1a). All other boundaries are no flow boundaries. While the geometry of the model resembles that of the exponential lumped parameter model, solute transport models require a dispersivity be assigned for numerical stability. A dispersivity of 0.5 m was used, which results in dispersion in the numerical simulations being driven primarily by variations in K (McCallum et al., 2014). To assess the impacts of heterogeneous hydraulic conductivities, the  $^3\text{H}$  activities and mean transit times from four sets of 30 simulations with an average K of  $1 \text{ m day}^{-1}$  and variances of K ( $\sigma^2 \ln(K)$ ) of 0.3, 1.0, 2.5, and 4.0 (Fig. S2) were compared to a model with homogeneous K. The FEFLOW simulations used time steps of 5 days over 65 years from 1950 to 2015. The relatively short time step ensured model stability and minimised numerical dispersion. Both  $^3\text{H}$  activities and age were simulated as solutes. The annual  $^3\text{H}$  activities of Melbourne rainfall (Tadros et al., 2014) interpolated onto the time steps of the model (Fig. S1b) were used as the  $^3\text{H}$  activity of recharge. Age was simulated by setting a constant age = 0 years for the upper boundary and calculating the travel time to the model outlet. For all simulations, the mean age and mean  $^3\text{H}$  activity are the flux weighted arithmetic means at the model outlet.

## 4. Results

### 4.1. Streamflow

The variations of streamflow at Noojee in the upper Latrobe catchment are typical of streams in this region. High streamflows are recorded in winter and lowest streamflows at the end of summer (Fig. 2b). The April 2015 and March 2016 samples represent the 82<sup>nd</sup> and 87<sup>th</sup> streamflow percentiles, respectively, between

1990 and 2016 (Fig. 2a). The August 2015 samples represent the 20<sup>th</sup> percentile of streamflow and the November 2015 samples the 65<sup>th</sup> percentile (Fig. 2a).

Runoff coefficients were estimated using streamflow records from between 1990 and 2016, where available (Department of Environment Land Water and Planning, 2017; Melbourne Water, 2017). For the Tooronga River, streamflow records between 1969 and 1986, which represents all available data for this site, were used. These multi-year periods encompass several high rainfall and drought years (Bureau of Meteorology, 2017), allowing long-term average runoff coefficients to be determined. Rainfall totals probably vary across the region and there is insufficient data to calculate the rainfall totals for each subcatchment. Hence, it was assumed that the rainfall was between the minimum and maximum average annual values in the upper Latrobe (1100–1400 mm) and upper Yarra catchments (750–1000 mm) as a whole. Runoff coefficients range from 18–23% (Lower Loch subcatchment) to 40–53% (Stringybark subcatchment) (Table 1).

#### 4.2. Tritium activities

The <sup>3</sup>H activity of the rainfall sample from Yarra Junction is 2.76 TU, which is within the expected range of average annual rainfall <sup>3</sup>H activities in this region of 2.6–3.0 TU interpolated from the data of Tadros et al. (2014) (Fig. 3). The <sup>3</sup>H activity of the Yarra Junction rainfall is also similar to those of a 9 month rainfall sample from Melbourne collected in July 2013 (<sup>3</sup>H = 2.72 TU) and three 9–17 month rainfall samples from Mount Buffalo in northeast Victoria (<sup>3</sup>H = 2.8–2.99 TU) (Cartwright and Morgenstern, 2015, 2016a). The <sup>3</sup>H activities of the streams are between 1.26 and 1.99 TU (Fig. 3), which are similar to <sup>3</sup>H activities of headwater streams in northeast Victoria (<sup>3</sup>H = 1.6–2.5 TU; Cartwright and Morgenstern, 2015, 2016a) and central Victoria (<sup>3</sup>H = 0.2–2.9 TU; Cartwright and Morgenstern, 2016b; Howcroft et al., 2017).

In the two low streamflow sampling rounds (April 2015 and March 2016), the streams from the upper Yarra catchment have lower <sup>3</sup>H activities (median = 1.44 TU, mean = 1.43 ± 0.11 TU, n = 12) than those from the upper Latrobe catchment (median = 1.55 TU, mean = 1.58 ± 0.09 TU, n = 8). The p values from two-tailed t tests are 0.004, implying that the difference between these two populations is significant beyond the 99 confidence interval. The <sup>3</sup>H activities in each of the subcatchments generally increase with increasing streamflow in the winter months (Fig. 3a and b). However, even at the highest streamflows, the <sup>3</sup>H activities are invariably lower than the <sup>3</sup>H activities of rainfall. Rather, <sup>3</sup>H activities

of between 1.6 and 2.0 TU are reached at moderate streamflows but not subsequently exceeded.

#### 4.3. Catchment attributes

Table 1 summarises catchment attributes derived from the GIS data. Drainage densities are between 0.93 and 1.04 km km<sup>-2</sup> and vary little either within or between the upper Latrobe and upper Yarra catchments. Likewise, there is little systematic difference between the mean or maximum distances to the stream. The upper Yarra subcatchments have lower average slopes (12–15) than those in the upper Latrobe catchment (24–27%). There are also significant differences in the landuse between the two catchments. In the upper Latrobe subcatchments, cleared land (i.e., that which is not occupied by forest) accounts for between 0 and 18% of the total area, while in the upper Yarra subcatchments it is between 85 and 99%.

#### 4.4. EC and major ion geochemistry

The EC of the upper Yarra streams varies between 113 and 606 μS cm<sup>-1</sup> (Table A1). The Wandin Yallock and Stringybark streams have the highest EC values (373–606 and 323–472 μS cm<sup>-1</sup>, respectively). The upper Latrobe streams have EC values of 45–97 μS cm<sup>-1</sup> and there is little difference between the subcatchments (Table A1). Na is the most common cation in the stream water (62–91% of all cations on a molar basis) with Ca (3–15%), Mg (1–24%), and K (1–11%) present in lower abundances (Table A1). Cl is the most abundant anion (81–98% on a molar basis) of those that were measured (Table A1); however, HCO<sub>3</sub> concentrations were not determined. The rainfall sample from Yarra Junction has a Na concentration of 1.2 mg l<sup>-1</sup> and an EC value of 21.6 μS cm<sup>-1</sup> (Table A1, Figs. 4 and 5). This is similar to non-coastal rainfall elsewhere in southeast Australia that has Na concentrations of 1–2 mg l<sup>-1</sup> and EC values of 15–30 μS cm<sup>-1</sup> (Blackburn and McLeod, 1983; Crosbie et al., 2012; Cartwright et al., 2014; Cartwright and Morgenstern, 2015, 2016a).

The EC values and major ion concentrations of rainfall are significantly lower than those of the river water at all streamflows (Table A1, Figs. 4 and 5). Unlike catchments elsewhere in southeast Australia (Cartwright and Morgenstern, 2015, 2016a,b; Howcroft et al., 2017), major ion concentrations in most of the upper Latrobe and Yarra catchments do not vary systematically with streamflow or <sup>3</sup>H activities (Table A1, Figs. 4 and 5). There is also little systematic variation in EC and streamflow collected as part of periodic stream salinity monitoring at Noojee (Fig. 4b). The higher EC values

**Table 1**  
Catchment attributes.

Site	Area km <sup>2</sup>	Drainage Density km <sup>-1</sup>	Slope %	Cleared land %	Max dist. <sup>a</sup> km	Mean dist. <sup>a</sup> km	Runoff Coefficient %
<i>Latrobe Catchment</i>							
Gentle Annie	63.8	0.98	24.27	0	1.21	0.31	28–35 <sup>b</sup>
Tooronga	62.1	1.00	25.32	1	1.12	0.30	41–52
Upper Loch	66.4	1.00	26.64	1	1.03	0.31	ne <sup>c</sup>
Lower Loch	114.2	0.99	26.31	5	1.18	0.32	18–23
Noojee	287.9	0.98	23.98	11	1.21	0.31	23–29
Willow Grove	559.0	1.00	24.06	18	1.21	0.31	23–29
<i>Yarra Catchment</i>							
Stringybark	8.7	0.98	11.98	99	0.89	0.30	40–53
Wandin	32.0	0.93	11.33	99	1.00	0.32	25–33
Cockatoo	49.2	1.00	15.65	95	1.14	0.29	20–26
Woori Yallock	323.4	1.04	14.78	85	1.19	0.29	19–25

<sup>a</sup> Maximum and mean distances to the stream.

<sup>b</sup> Range calculated for maximum and minimum estimates of annual rainfall in the catchment.

<sup>c</sup> ne = not estimated.

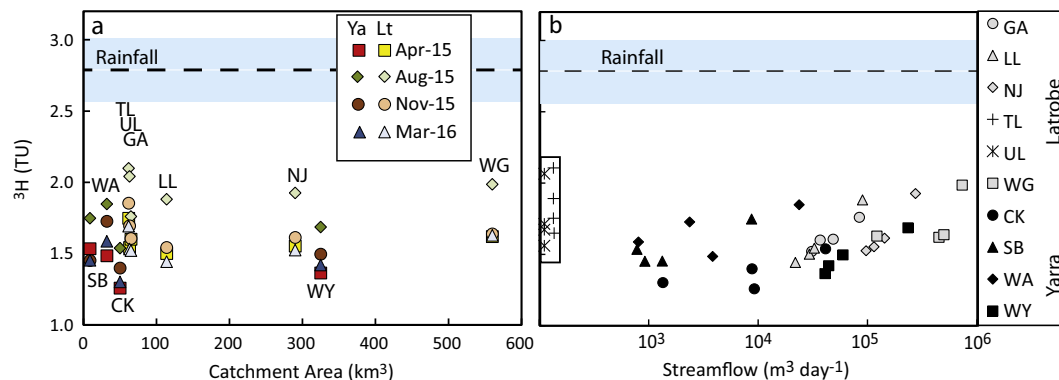


**Fig. 3.** (a).  $^3\text{H}$  activities vs. catchment area for the upper Latrobe (Lt) and Yarra (Ya) catchments in the different sampling rounds. (b). Variations in  $^3\text{H}$  activities with streamflow in the individual catchments (no streamflow data is available for Tooronga or Upper Loch). Dashed line is the  $^3\text{H}$  activity of the Yarra Junction rainfall sample. Shaded box is the interpolated range of average annual rainfall  $^3\text{H}$  activities from Tadros et al., (2014). Data from Table A1. Abbreviations: GA = Gentle Annie; LL = Lower Lock; NJ = Noojee; TL = Tooronga; UL = Upper Loch; WG = Willowgrove; CK = Cockatoo; SB = Stringybark; WA = Wandin Yallock; WY = Woori Yallock.

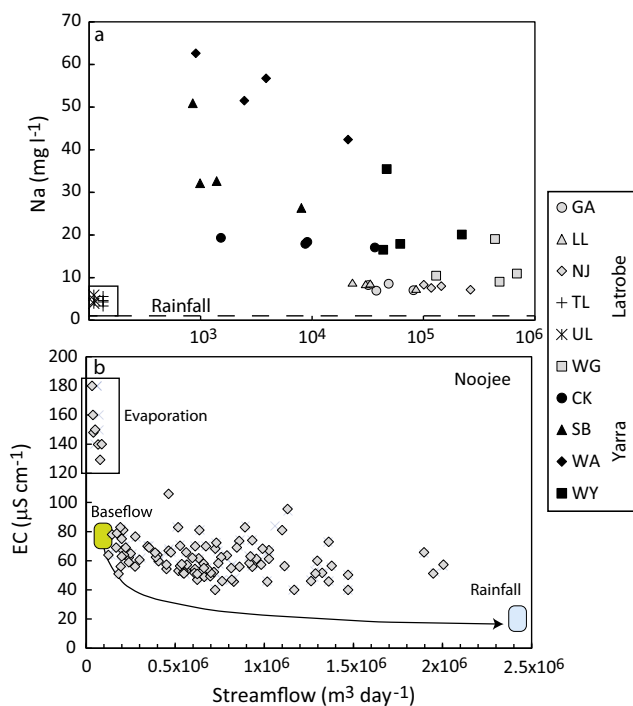


**Fig. 4.** (a). Variations Na concentrations with streamflow in the individual catchments (no streamflow data is available for Tooronga or Upper Loch). Rainfall is the composition of the Yarra Junction rainfall sample. Data from Table A1. Abbreviations: GA = Gentle Annie; LL = Lower Lock; NJ = Noojee; TL = Tooronga; UL = Upper Loch; WG = Willowgrove; CK = Cockatoo; SB = Stringybark; WA = Wandin Yallock; WY = Woori Yallock. (b). Variations in EC values with streamflow at Noojee (Data from Department of Environment Land Water and Planning (2017)). The arrowed trend depicts the predicted EC vs streamflow trend for dilution of baseflow (assumed to have an EC value typical of the stream at low streamflows) with rainfall that has EC values typical of non-coastal rainfall in southeast Australia (e.g., Blackburn and McLeod, 1983; Crosbie et al., 2012; Cartwright and Morgenstern, 2015, 2016a,b) constructed following Godsey et al. (2009) and Cartwright and Morgenstern (2015).

at low streamflows probably reflect in-stream evaporation during summer; however, generally, the EC values vary between 40 and 80  $\mu\text{S cm}^{-1}$  for streamflows that range over several orders of magnitude.

Molar Na/Cl ratios of the stream water vary from 0.6 to 1.3 with higher Na/Cl ratios recorded in the waters with lower Cl concentrations (Fig. 6a). Na/Cl ratios that are higher than those of local rain-

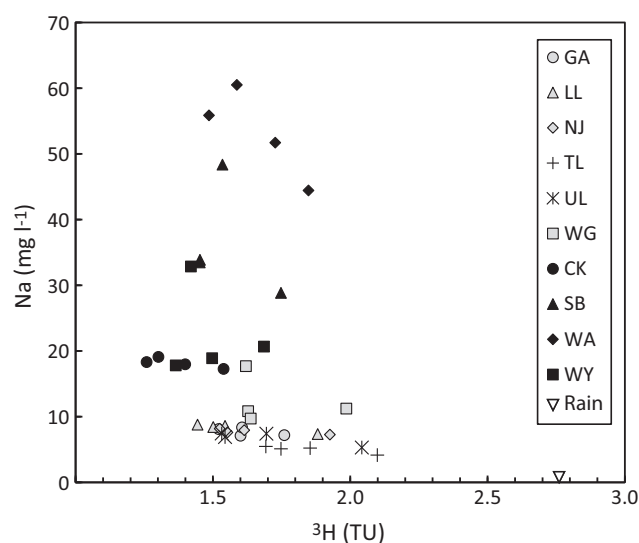


**Fig. 5.** Na concentrations vs.  $^3\text{H}$  activities for the individual catchments and the Yarra Junction rainfall sample (data from Table A1). Abbreviations: GA = Gentle Annie; LL = Lower Lock; NJ = Noojee; TL = Tooronga; UL = Upper Loch; WG = Willowgrove; CK = Cockatoo; SB = Stringybark; WA = Wandin Yallock; WY = Woori Yallock.

fall (typically 0.8–1.1) reflect weathering of silicate minerals such as feldspar (Herczeg et al., 2001; Tweed et al., 2005; Cartwright and Morgenstern, 2015, 2016a). However, the observation that Na/Cl ratios do not far exceed those of rainfall implies that silicate dissolution is limited. The Na/Cl ratios of some more saline waters are lower than those of rainfall (Fig. 6a), which is probably due to Na-Ca exchange on clay minerals (Tweed et al., 2005). Molar Cl/Br ratios of 490–835 (Fig. 6b) span those of the oceans and rainfall in southeast Australia but are far below those expected if halite or anthropogenic salts (e.g. fertilisers) had been dissolved (Herczeg et al., 2001; Cartwright et al., 2006). Overall, as is the case throughout southeast Australia (Allison et al., 1990; Herczeg et al., 2001; Tweed et al., 2005; Cartwright et al., 2006), the variations in the salinity of the stream water is driven by differences in evapotranspiration with minor impacts of weathering and ion exchange. This implies that the Wandin Yallock and Stringybark catchments have higher degrees of evapotranspiration, although (given that they have similar geology, vegetation, and rainfall to the other upper Yarra catchments), the causes of this are not clear.

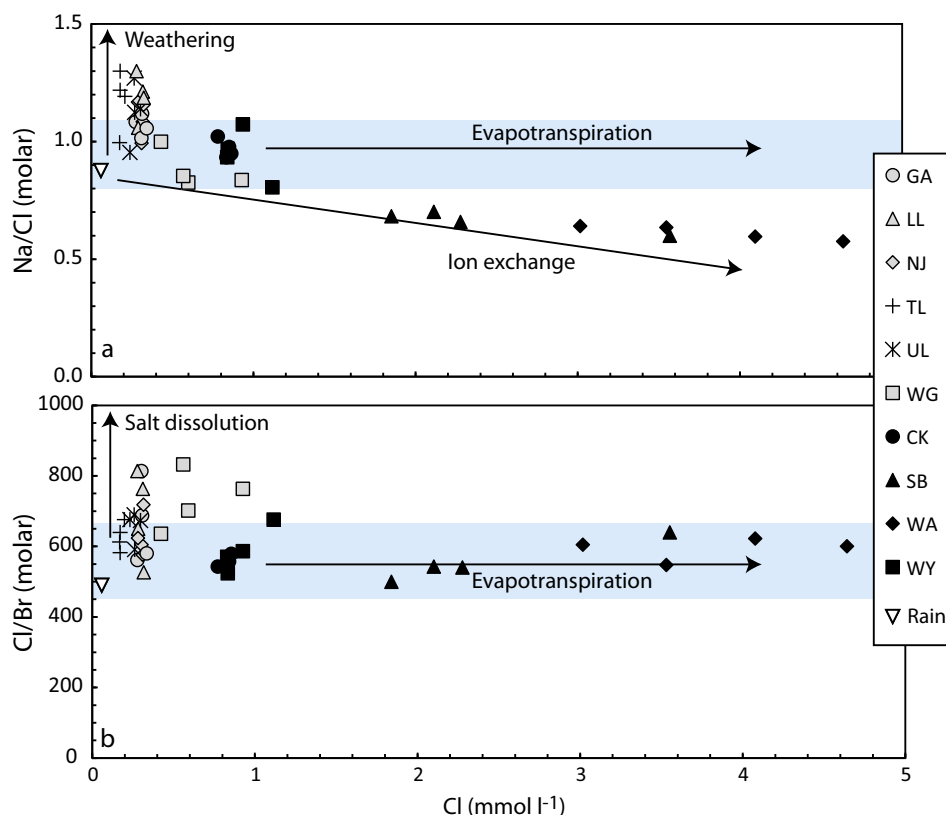


**Fig. 6.** Variations in Na/Cl (6a) and Cl/Br (6b) with Cl concentrations (data from Table A1). Overall weathering and salt (e.g., halite or anthropogenic sources of Cl) dissolution are minor. Shaded boxes are typical composition in non-coastal rainfall in southeast Australia (e.g., Blackburn and McLeod, 1983; Herczeg et al., 2001; Cartwright et al., 2006, 2014; Crosbie et al., 2012; Cartwright and Morgenstern, 2015, 2016a,b).

#### 4.5. Modelled $^3\text{H}$ activities

The  $^3\text{H}$  activities at the outlet of the FEFLOW model generally decrease with depth (Fig. 7), which is a similar trend to that observed in the exponential lumped parameter model (e.g., Cook and Bohlke, 2000; Jurgens et al., 2012). Not surprisingly, the mean transit time of water correlates with the mean  $^3\text{H}$  activity at the model outlet (Fig. 8). The geometry of the FEFLOW model is similar to that of the exponential lumped parameter model. However, even for the homogeneous model, the mean transit times at any given  $^3\text{H}$  activity predicted from the FEFLOW model are longer (Fig. 8). This is due to the FEFLOW model incorporating dispersion, which is not present in the exponential lumped parameter model.

The mean transit times at the model outlet decrease as  $\sigma^2\ln(K)$  increases. The homogeneous model has a mean transit time of 72 years. Mean transit times for the other sets of simulations are:  $62.9 \pm 4.5$  years for  $\sigma^2\ln(K) = 0.3$ ;  $54.2 \pm 9.1$  years for  $\sigma^2\ln(K) = 1.0$ ;  $47.7 \pm 12.5$  years for  $\sigma^2\ln(K) = 2.5$ ; and  $50.5 \pm 13$  years for  $\sigma^2\ln(K) = 4.0$ . The decrease in mean transit times are due to the presence of interconnected high K pathways that become increasingly prevalent as  $\sigma^2\ln(K)$  increases. The variability of mean transit times also increases with increasing  $\sigma^2\ln(K)$ . For a  $^3\text{H}$  activity of 1.5 TU, the range of mean transit times are  $\sim 3$  years for  $\sigma^2\ln(K) = 0.3$  increasing to  $\sim 6$  years for  $\sigma^2\ln(K) = 4.0$ . For the whole range of simulations, the range in mean transit times at 1.5 TU is 10 years (Fig. 8).

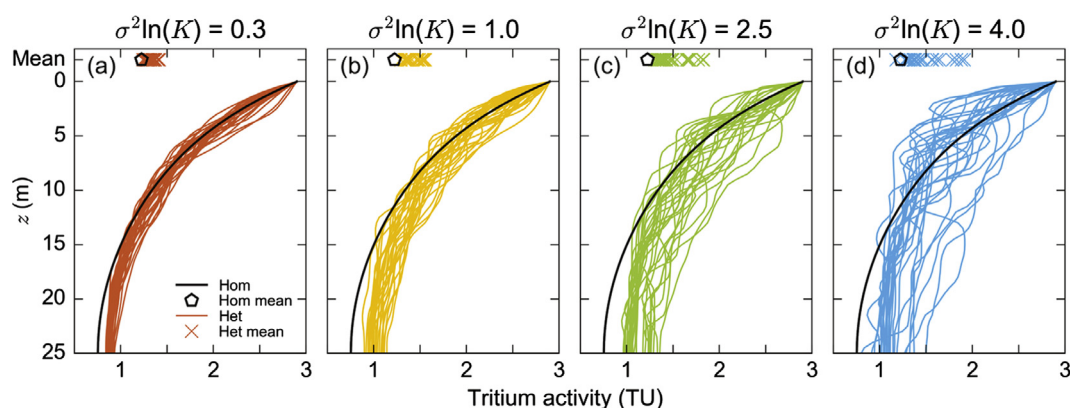


**Fig. 7.**  $^3\text{H}$  activities vs. depth at the model outlet for varying degrees of heterogeneity (Het) in K. Hom is the homogeneous FEFLOW model.



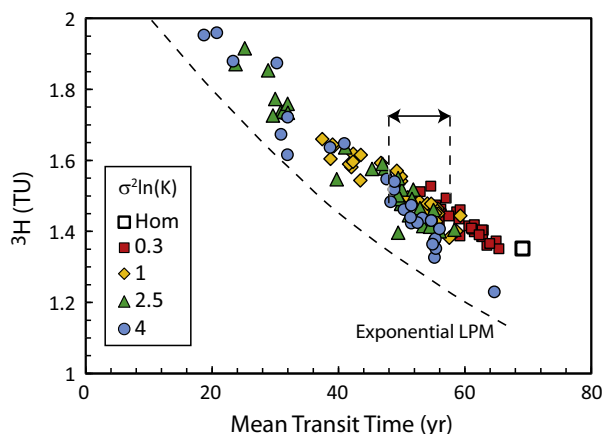


**Fig. 8.**  $^3\text{H}$  activities vs. mean transit times at the model outlet for varying degrees of heterogeneity in  $K$ . Hom is the homogeneous FEFLOW model. Arrowed line shows range of mean transit times for a  $^3\text{H}$  activity of 1.5 TU. Dashed line is the exponential mixing model from TracerLPM for reference.

## 5. Discussion

The combination of major ion geochemistry, streamflows,  $^3\text{H}$  activities, and catchment attributes allow aspects of the hydrogeology of the upper Latrobe and upper Yarra catchments to be understood. This section addresses the prime objectives of the study, namely: the range of mean transit times; whether mean transit times can be predicted from catchment attributes or geochemical data; and the uncertainties in the calculated mean transit times.

### 5.1. Changing stores of water at different streamflows

There is strong seasonality to southeast Australian rainfall (Bureau of Meteorology, 2017) and streams are generally dominated by baseflow during summer (Cartwright et al., 2014). Thus, baseflow probably contributes the vast majority of water to the streams in April 2015 and March 2016 when streamflows were low (Fig. 2). Higher winter streamflows can conceivably reflect the progressive mobilisation of shallower younger water stores (e.g., soil water or water from the regolith) as the catchment wets up (c.f. Hrachowitz et al., 2013) or mixing between baseflow and recent rainfall.

This study avoided collecting samples during the high flow events immediately following rainfall when direct input of recent rainfall to the stream may occur. The dilution of saline baseflow with recent rainfall also results in major ion concentrations or EC values being inversely correlated with streamflow (Godsey et al., 2009; Cartwright and Morgenstern, 2015), which is not observed in these catchments (Fig. 4). The predicted EC vs. streamflow trend for the situation where all the additional streamflows is derived from recent rainfall inputs also fails to replicate the observed EC values (Fig. 4b). Rather, as documented in similar catchments elsewhere in southeast Australia, the infiltrating rainfall has likely progressively mobilised the shallower stores of water from the soil or regolith (Cartwright and Morgenstern, 2015; Howcroft et al., 2017). These water stores almost certainly have shorter residence times than the deeper groundwater, which explains why  $^3\text{H}$  activities are higher in winter. Given that samples were not collected over the high flow peaks, the data does not preclude recent rainfall contributing to streamflow during individual high flow events.

### 5.2. Mean transit times

Based on the above conceptualisation of how the flow system responds to rainfall, mean transit times were calculated assuming that single flow system contributes to the stream at all flow conditions. If there were some inflow of recent rainfall, this approach yields the minimum transit time of the baseflow component. The estimated mean transit times calculated using the suite of lumped parameter models are between 7 and 62 years (Table 2, Fig. 9). The range of mean transit times from the various models increases with the  $^3\text{H}$  activity (Fig. 9a); however, the relative difference decreases. For example, mean transit times for a water with a  $^3\text{H}$  activity of 2 TU are between 9.6 and 14.2 years (or  $\pm 19\%$ ). For a water with a  $^3\text{H}$  activity of 1.5 TU, they are between 28.0 and 41.9 years ( $\pm 13\%$ ).

For the two low streamflow sampling periods, the mean transit times in the upper Yarra subcatchments are 28–62 years (April 2015) and 20–53 years (March 2016), whereas the mean transit times in the upper Latrobe subcatchments are 16–42 years (April 2015) and 16–41 years (March 2016). The Tooronga River in the upper Latrobe catchment has the shortest mean transit times (16–26 years) and Cockatoo Creek in the upper Yarra catchment has the longest mean transit times (42–62 years). At the higher streamflows, the mean transit times in the upper Latrobe subcatchments are 7–24 years (August 2015) and 13–36 years (November 2015). At the corresponding times, the mean transit times in the upper Yarra subcatchments are 13–37 years (August 2015) and 16–46 years (November 2015). As at low streamflows, the mean transit times are shortest in the Tooronga River (9–13 years in August 2015 and 13–20 years in November 2015) and longest at Cockatoo Creek (26–37 years in August 2015 and 37–46 years in November 2015).

### 5.3. Uncertainties

Propagating the analytical uncertainty in  $^3\text{H}$  activities (Table A1) results in uncertainties in mean transit times of 1–2 years. Compared with the other uncertainties, this has only a minor impact. Mixing of water with different mean transit times within a subcatchment (aggregation) results in calculated mean transit times being lower than the actual mean transit time (Suckow, 2014; Kirchner, 2016; Stewart et al., 2017). The aggregation error is difficult to assess but it reduces as an increasing number of waters are mixed. This is because flow systems where numerous aliquots of water with different mean transit times mix are similar to what is described by the lumped parameter models. For example, using similar lumped parameter models and input functions to this study, Cartwright and Morgenstern (2016a) estimated the aggregation error resulting from an equal mixture of two waters with mean transit times of 10 and 50 years was approximately 13%. However, if several waters with mean transit times of between 10 and 50 years mixed, the aggregation errors were significantly lower.

The impacts of uncertainties in the  $^3\text{H}$  activities of rainfall may be illustrated using the exponential-piston flow model with an EPM ratio of 1 (almost identical results are produced by the other models). The assumed  $^3\text{H}$  activity of modern rainfall makes relatively little difference to the estimated mean transit time (Fig. 9b). Varying the modern rainfall  $^3\text{H}$  activities between 2.6 and 3.0 TU (which is the likely range of rainfall  $^3\text{H}$  activities in this region of southeast Australia: Tadros et al., 2014) produces a range of mean transit times of 3 years for a  $^3\text{H}$  activity of 2 TU and  $<0.1$  year for a  $^3\text{H}$  activity of 1.5 TU. Uncertainties in the  $^3\text{H}$  activities of past rainfall exert a greater influence on the mean transit times. Fig. 9c illustrates the impact of varying the  $^3\text{H}$  activity of rainfall by  $\pm 10\%$ , which is approximately the relative uncertainty in mod-

**Table 2**

Estimated mean transit times.

Sample	EMM <sup>b</sup> yr	EPF (0.3) yr	EPF (1) yr	DM (0.1) yr	DM (1) yr
<b>7/04/2015</b>					
Willow Grove (LT) <sup>a</sup>	31.7	28.1	22.2	21.2	32.8
Noojee (LT)	35.3	31.3	26.2	36.8	37.2
Tooronga (LT)	25.4	21.2	16.8	16.0	25.6
Upper Loch (LT)	35.8	31.8	26.9	38.0	37.8
Lower Loch (LT)	38.2	34.0	30.9	41.9	40.9
Gentle Annie (LT)	32.8	29.0	23.1	22.7	34.0
Woori Yallock (Y)	46.6	41.4	45.9	49.4	51.8
Cockatoo (Y)	54.1	47.6	56.2	53.9	62.0
Wandin (Y)	39.1	34.7	32.6	42.9	42.0
Stringybark (Y)	36.3	32.2	27.7	39.0	38.4
<b>12/08/2015</b>					
Willow Grove (LT)	13.9	10.8	9.9	10.1	14.7
Noojee (LT)	16.3	12.6	11.6	11.4	16.9
Tooronga (LT)	10.0	8.2	7.3	7.7	11.1
Upper Loch (LT)	11.8	9.4	8.5	8.9	12.9
Lower Loch (LT)	18.3	14.1	13.2	12.3	18.6
Gentle Annie (LT)	23.9	19.4	15.9	15.2	24.1
Woori Yallock (Y)	27.5	23.2	18.3	17.3	27.9
Cockatoo (Y)	35.1	31.1	25.6	33.9	36.9
Wandin (Y)	19.8	15.4	13.9	13.1	20.0
Stringybark (Y)	24.5	20.0	16.3	15.5	24.7
<b>18/11/2015</b>					
Willow Grove (LT)	29.2	24.8	19.7	18.5	29.8
Noojee (LT)	30.4	26.2	20.9	19.6	31.2
Tooronga (LT)	18.9	14.5	13.3	12.6	19.2
Upper Loch (LT)	26.4	21.7	17.5	16.6	26.6
Lower Loch (LT)	34.1	30.1	24.3	24.9	35.6
Gentle Annie (LT)	30.8	26.6	21.4	19.9	31.7
Woori Yallock (Y)	36.8	32.4	27.4	37.7	38.8
Cockatoo (Y)	42.6	37.5	36.8	45.6	46.2
Wandin (Y)	24.8	20.1	16.5	15.7	25.0
Stringybark (Y)	39.4	34.7	31.5	42.1	42.1
<b>30/03/2016</b>					
Willow Grove (LT)	28.8	24.0	19.2	18.2	29.4
Noojee (LT)	34.2	29.8	24.3	24.5	35.7
Tooronga (LT)	25.6	20.6	17.0	16.1	25.9
Upper Loch (LT)	33.8	29.4	23.9	23.7	35.2
Lower Loch (LT)	38.9	34.1	30.0	40.5	41.1
Gentle Annie (LT)	34.5	30.0	24.5	24.0	36.0
Woori Yallock (Y)	40.2	35.3	32.1	42.6	43.2
Cockatoo (Y)	48.0	41.9	44.2	49.6	53.3
Wandin (Y)	30.9	26.3	21.1	20.0	31.8
Stringybark (Y)	38.3	33.6	29.1	39.7	40.7

<sup>a</sup> LT = Latrobe catchment; Y = Yarra catchment.<sup>b</sup> Lumped parameter models: EMM = Exponential flow model, EPF = exponential-piston flow model (EPM ratio in brackets); DM = dispersion model (DP in brackets).

ern rainfall  $^3\text{H}$  activities (Tadros et al., 2014). For a  $^3\text{H}$  activity of 1.5 TU, the range of mean transit times is approximately 13.5 years, a relative uncertainty of  $\pm 18\%$ .

The calculations used average annual rainfall  $^3\text{H}$  activities as the input function. However, if summer rainfall is lost by evapotranspiration, the  $^3\text{H}$  activities of the recharging water may be different (Morgenstern et al., 2010; Blavoux et al., 2013). The monthly variation of  $^3\text{H}$  activities in Melbourne (International Atomic Energy Agency, 2017) are similar to those at Kiatoke, New Zealand, for which there is a more detailed record (Morgenstern et al., 2010). The monthly variation in rainfall  $^3\text{H}$  activities in any given year is  $<1$  TU and the  $^3\text{H}$  activities in summer rainfall are close to the average annual  $^3\text{H}$  activities. This is also implied by the observation that the  $^3\text{H}$  activity of summer (December to February) rainfall at Mount Buffalo (northeast Victoria) was closely similar (2.86 TU) to that of two annual rainfall samples (2.99 and 2.85 TU) (Cartwright and Morgenstern, 2015). With such a seasonal distribution of  $^3\text{H}$  activities, the uncertainties resulting from using the average annual  $^3\text{H}$  activity are minor (c.f., Morgenstern et al., 2010).

The FEFLOW simulations highlight another uncertainty in calculating mean transit times. Lumped parameter models have the advantage of not requiring a detailed knowledge of aquifer properties (such as hydraulic conductivities) that are difficult to obtain; however, it is highly unlikely in reality that hydraulic conductivities are homogeneous. For aquifers with layers of different lithologies, binary (or higher order) lumped parameter models may be used (Maloszewski and Zuber, 1982; Maloszewski, 2000). However, the hydraulic conductivities are still likely to vary within each of the layers.

In the FEFLOW simulations with highly heterogeneous hydraulic conductivities, there is increasing variability in the relationship between mean transit times and  $^3\text{H}$  activities, and the  $^3\text{H}$  activity vs. depth profiles are irregular (Figs. 7 and 8). The range of mean transit times estimated for a  $^3\text{H}$  activity of 1.5 TU in the FEFLOW simulations is 10 years (Fig. 8). This is a relative uncertainty of  $\pm 13\%$ , which is similar to other uncertainties discussed above. The FEFLOW model includes dispersion, which results in the mean transit times at any  $^3\text{H}$  activity being longer to those calculated from the lumped parameter models. These differences highlight

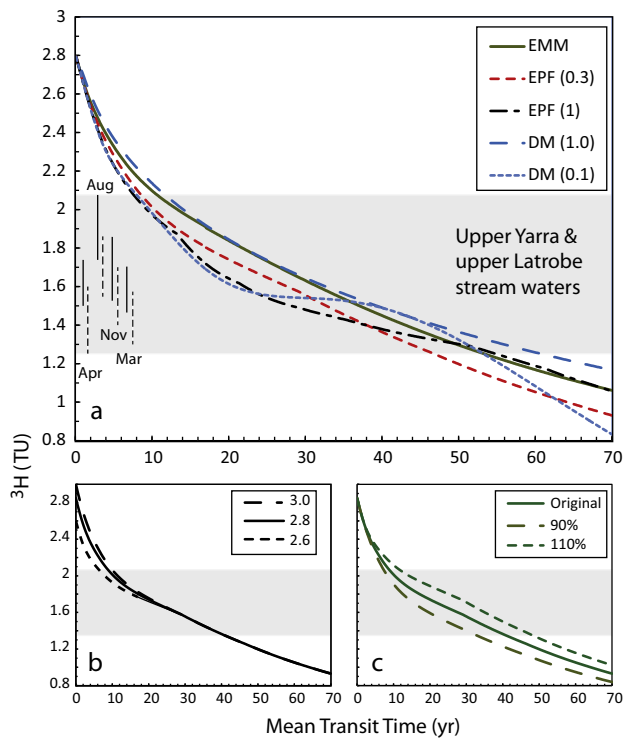


**Fig. 9.** (a). Mean transit times vs.  $^3\text{H}$  activities (Tables A1, 2) calculated using the lumped parameter models discussed in the text. EMM = Exponential Model; EPF = Exponential-Piston Flow Model (EPM ratio in brackets); DM = Dispersion Model (DP in brackets). The shaded area depicts the range of  $^3\text{H}$  activities in the upper Latrobe and Yarra streams. Ranges of  $^3\text{H}$  activities for the upper Latrobe (solid lines) and Yarra (dashed lines) catchments for April 2015, August 2015, November 2015, and March 2016 also indicated. (b). Impacts of varying  $^3\text{H}$  activity of modern rainfall from 2.6 to 3.0 TU on mean transit time calculated using the Exponential-Piston Flow Model (EPF = 0.33). (c). Impacts of varying  $^3\text{H}$  activity of rainfall between 90 and 110% of its assumed values on mean transit time calculated using the Exponential-Piston Flow Model (EPF = 0.33).

the uncertainties that stem from adopting lumped parameter models with simple geometries (c.f. Weissmann et al., 2002; McCallum et al., 2014, McCallum et al., 2015).

If uncertainties are uncorrelated and have Gaussian distributions, the overall uncertainty is the square root of the sum of the squares of the individual uncertainties. The main uncertainties outlined above (the choice of the lumped parameter model, aggregation, errors in the assumed  $^3\text{H}$  input, and the presence of a heterogeneous hydrogeological conductivity) are all approximately  $\pm 15\%$ , which would imply an overall uncertainty in mean transit times of approximately  $\pm 30\%$ . While this is considerable, the conclusion that the mean transit times are years to decades long is still valid.

Relative differences in mean transit times within or between catchments are more readily assessed. The subcatchments may have flow paths with different geometries or different degrees of heterogeneity of hydraulic conductivity, which affects the comparison of mean transit times between subcatchments. However, if the geometry of the flow paths in an individual subcatchment are similar during wetter and drier periods and the hydraulic conductivities do not change, relative differences in mean transit times at different streamflows in the same subcatchment are more robustly calculated. The  $^3\text{H}$  activities of rainfall are probably closely similar over areas the size of the study area (e.g., Tadros et al., 2014). Again this allows the relative differences in mean transit times at different streamflows in the same subcatchment to be more readily assessed. By contrast, aggregation may affect

the comparison of mean transit times both between subcatchments and within the same subcatchment at different streamflows if different stores of water are mobilised.

#### 5.4. Predicting mean transit times

Table 3 and Fig. 10 summarises correlation coefficients between catchment attributes (Table 1) and the  $^3\text{H}$  activities at the low streamflow conditions in April 2015 (Table A1). Because  $^3\text{H}$  activities are directly related to mean transit times, correlations between catchment attributes and mean transit times are similar. Correlation coefficients are considered to be strong at  $R^2 \geq 0.75$ , moderate at  $0.75 > R^2 > 0.5$ , and weak at  $R^2 \leq 0.5$ . There are few strong correlations (Table 3, Fig. 10). The  $^3\text{H}$  activities and the runoff coefficient are weakly correlated ( $R^2 = 0.37$ ) for the dataset as a whole but have moderate to strong correlations ( $R^2 = 0.65$ – $0.90$ ) within the two catchments. Slopes and  $^3\text{H}$  activities have a strong negative correlation in the upper Yarra subcatchments ( $R^2 = 0.88$ ) but have weak negative correlations ( $R^2 = 0.08$ ) in the upper Latrobe subcatchments and a weak positive correlation ( $R^2 = 0.32$ ) across the two catchments. There is a weak negative correlation between the proportion of cleared land and  $^3\text{H}$  activities ( $R^2 = 0.46$ ) in the dataset as a whole and in the two individual catchments ( $R^2 = 0.1$ – $0.27$ ). Drainage densities are weakly correlated with  $^3\text{H}$  activities both within ( $R^2 = 0.31$ – $0.15$ ) and across ( $R^2 = 0.03$ ) the two catchments. Both the maximum and mean distances are have strong negative correlations with  $^3\text{H}$  activities in one of the catchments ( $R^2 = 0.75$  and  $0.81$ ), but are not correlated across the two catchments ( $R^2 = 0.00$  and  $0.17$ ).

Overall there are no strong correlations between most catchment attributes  $^3\text{H}$  activities that apply in both catchments or across the two catchments. The correlation between runoff coefficients and  $^3\text{H}$  activities are stronger, especially within the catchments. The same range of factors that control the mean transit times probably control the runoff coefficient. For example, catchments with high evapotranspiration rates will have lower rates of recharge that result in longer mean transit times and lower runoff coefficients. Thus, as is the case elsewhere in southeast Australia (Cartwright and Morgenstern, 2015), the runoff coefficient may be a plausible proxy for mean transit times for streams in the same catchment.

There are multiple interacting factors that control the transmission of water through catchments (e.g., as discussed by McGuire et al., 2005; McGuire and McDonnell, 2006; Soulsby et al., 2009; Hrachowitz et al., 2009a, 2009b; 2010; 2013; Lachassagne et al., 2011). In addition to the geomorphology and geometry of the catchments, the hydraulic properties of the soils and underlying rocks together with variations in the degree of evapotranspiration are also important. Because clearing of eucalypt vegetation in southeast Australia was commonly followed by an increase in recharge (Allison et al., 1990; Cartwright et al., 2006), it was antic-

**Table 3**  
Correlation coefficients between catchment attributes and  $^3\text{H}$  activities.

Catchment Attribute	Combined <sup>a</sup>	Yarra	Latrobe
Area	0.01 <sup>b</sup>	0.12	0.00
Slope	0.32	<b>0.88</b>	0.08
Max dist.	0.00	<b>0.75</b>	0.00
Mean dist.	0.17	0.43	<b>0.81</b>
Drainage density	0.03	0.31	0.15
% Cleared land	0.46	0.01	0.27
Runoff coefficient <sup>c</sup>	0.37	0.65	<b>0.90</b>

<sup>a</sup> Correlations across both catchments.

<sup>b</sup>  $R^2$  values. Positive correlations in plain type, negative correlations in *italics*, strong correlations ( $R^2 \geq 0.75$ ) in **bold**.

<sup>c</sup> Average value from Table 2 assumed.

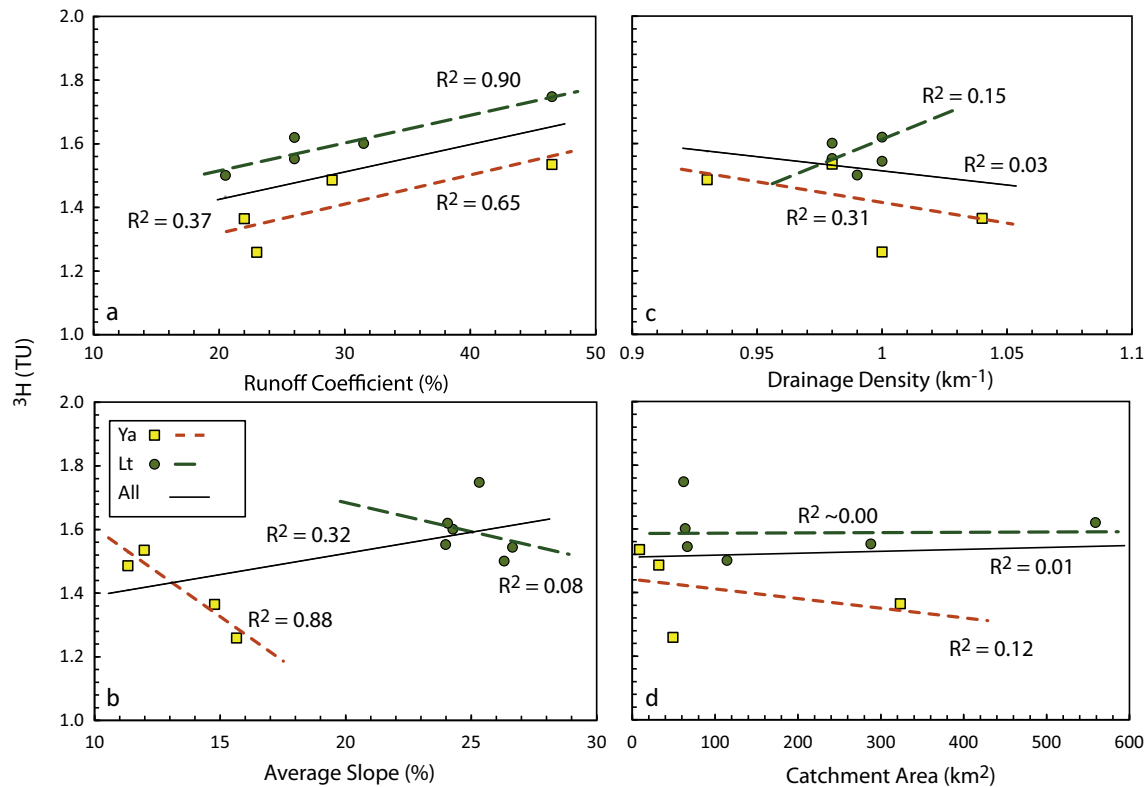


**Fig. 10.** Correlations between  $^3\text{H}$  activities in April 2015 and the average runoff coefficient (10a), average slope (10b), drainage density (10c), and catchment area (10d). Data from Table A1 and Table 1. Correlation coefficients are shown for the Yarra (Ya) and Latrobe (Lt) subcatchments and the data as a whole (All).

ipated that the mean transit times in the cleared Yarra catchment would be shorter than those in the Latrobe catchment, which is dominated by native forests. However, this was not observed. Other differences between the two catchments (e.g., geology, rainfall, and possibly soil types) may have more impact than differences in land use. Thus, while land clearing may have reduced mean transit times in the Yarra catchment, this is not apparent by comparison with adjacent catchments.

In other catchments in southeast Australia and elsewhere, major ion concentrations may be used as a proxy for  $^3\text{H}$  activities (Morgenstern et al., 2010; Cartwright and Morgenstern 2015, 2016a,b; Beyer et al., 2016; Howcroft et al., 2017). The major ion concentrations in the upper Latrobe subcatchments are generally lower than those in the Yarra subcatchments, which broadly reflects the differences in  $^3\text{H}$  activities. In detail, however, major ion concentrations and  $^3\text{H}$  activities are poorly correlated (e.g., Fig. 5). The lack of correlation may be due to different weathering reactions occurring at different localities in the catchments and evapotranspiration rates being spatially variable. Correlations within individual subcatchments at different streamflows are locally stronger. For example,  $R^2$  values for the correlation between Na and  $^3\text{H}$  are up to 0.96 in the upper Latrobe subcatchments and up to 0.72 in the upper Yarra subcatchments. This may allow the major ion geochemistry to be used as a proxy for  $^3\text{H}$  at different streamflows in individual subcatchments.

## 6. Summary and conclusions

Calculating precise mean transit times is difficult due to a range of uncertainties, and characterising a catchment in sufficient detail to reduce some of these uncertainties would be difficult. However, estimating broad ranges of mean transit times is feasible. Additionally, determining the variation in mean transit times at different

streamflows within the same subcatchment is more easily achieved than comparing mean transit times between subcatchments. The conclusion that the mean transit times at baseflow conditions are several years to decades in both the upper Yarra and upper Latrobe catchments is robust and is vital information for catchment management. Firstly, it suggests that there is a long-lived store of water in these catchments that can sustain streamflow during drought periods. Additionally, the long mean transit times may result in considerable delay in contaminants reaching the streams via the groundwater. In the Yarra catchment, agriculture, local housing developments, and small-scale industries are potential sources of contaminants (particularly nitrate).

That it was not possible to reliably predict  $^3\text{H}$  activities from individual catchment attributes (including a major difference in landuse) or the major ion geochemistry limits our ability to make first-order predictions of mean transit times in similar catchments or at different times. The runoff coefficient, which has proven to be a reasonable indicator of mean transit times elsewhere in southeast Australia (Cartwright and Morgenstern, 2015), provided the most reliable prediction of mean transit times. This is probably due to both the runoff coefficient and mean transit times reflecting recharge rates and rates of groundwater flow within the catchments. Mean transit times are likely controlled by the interaction of catchment attributes such as slope or drainage density, the hydraulic properties of the soils, regolith, and aquifers, and evapotranspiration rates. Characterising hydraulic properties or evapotranspiration across a whole catchment would be difficult and understanding how the various attributes combine to control mean transit times is also difficult.

The mean transit times in the upper Yarra and Latrobe catchments are years to decades. Similar mean transit times are documented elsewhere in Australia (Cartwright and Morgenstern, 2015, 2016a, 2016b; Duvert et al., 2016; Howcroft et al., 2017)



and New Zealand (Morgenstern et al., 2015). However, mean transit times in catchments elsewhere appear to be only a few years (e.g., McGuire and McDonnell, 2006; Hrachowitz et al., 2009a,b; Speed et al., 2010). It is not clear whether the differences in mean transit times relates to differences in climate, depth of weathering, vegetation types, soil properties, or relief. This together with the challenge in predicting mean transit times illustrates the difficulties in generalising upper catchment behaviour on a global scale.

## Acknowledgements

Monash University and the National Centre for Groundwater Research and Training (NCGRT) provided funding for this project. The NCGRT was supported through Special Research Initiative SR0800001 funded by the Australian Research Council and the National Water Commission. We also thank DHI for providing the FEFLOW license through the NCGRT. Massimo Raveggi and Rachael Pearson helped with the geochemical analyses at Monash University. The perceptive comments of two anonymous reviewers helped improve the paper.

## Appendix A. Supplementary data

Supplementary data associated with this article can be found, in the online version, at <https://doi.org/10.1016/j.jhydrol.2017.12.007>.

## References

- Allison, G.B., Cook, P.G., Barnett, S.R., Walker, G.R., Jolly, I.D., Hughes, M.W., 1990. Land clearance and river salinisation in the western Murray Basin, Australia. *J. Hydrol.* 119, 1–20. [https://doi.org/10.1016/0022-1694\(90\)90030-2](https://doi.org/10.1016/0022-1694(90)90030-2).
- Beyer, M., Jackson, B., Daughney, C., Morgenstern, U., Norton, K., 2016. Use of hydrochemistry as a standalone and complementary groundwater age tracer. *J. Hydrol.* 543, 127–144. <https://doi.org/10.1016/j.jhydrol.2016.05.062>.
- Blackburn, G., McLeod, S., 1983. Salinity of atmospheric precipitation in the Murray Darling Drainage Division, Australia. *Aust. J. Soil Res.* 21, 400–434. <https://doi.org/10.1071/SR9830411>.
- Blavoux, B., Lachassagne, P., Henriot, A., Ladouche, B., Marc, V., Beley, J.-J., Nicoud, G., Olive, P., 2013. A fifty-year chronicle of tritium data for characterising the functioning of the Evian and Thonon (France) glacial aquifers. *J. Hydrol.* 494, 116–133. <https://doi.org/10.1016/j.jhydrol.2013.04.029>.
- Böhlke, J.K., Michel, R.L., 2009. Contrasting residence times and fluxes of water and sulfate in two small forested watersheds in Virginia, USA. *Sci. Total Environ.* 407, 4363–4377. <https://doi.org/10.1016/j.scitotenv.2009.02.007>.
- Bureau of Meteorology, 2017. Commonwealth of Australia Bureau of Meteorology. [www.bom.gov.au](http://www.bom.gov.au).
- Cartwright, I., Giffedder, B., Hofmann, H., 2014. Contrasts between estimates of baseflow help discern multiple sources of water contributing to rivers. *Hydrol. Earth Syst. Sci.* 18, 15–30. <https://doi.org/10.5194/hess-18-15-2014>.
- Cartwright, I., Hofmann, H., Sirianos, M.A., Weaver, T.R., Simmons, C.T., 2011. Geochemical and  $^{222}\text{Rn}$  constraints on baseflow to the Murray River, Australia, and timescales for the decay of low-salinity groundwater lenses. *J. Hydrol.* 405, 333–343. <https://doi.org/10.1016/j.jhydrol.2011.05.030>.
- Cartwright, I., Morgenstern, U., 2015. Transit times from rainfall to baseflow in headwater catchments estimated using tritium: The Owens River, Australia. *Hydrol. Earth Syst. Sci.* 19, 3771–3785. <https://doi.org/10.5194/hess-19-3771-2015>.
- Cartwright, I., Morgenstern, U., 2016a. Contrasting transit times of water from peatlands and eucalypt forests in the Australian Alps determined by tritium: implications for vulnerability and the source of water in upland catchments. *Hydrol. Earth Syst. Sci.* 20, 4757–4773. <https://doi.org/10.5194/hess-20-4757-2016>.
- Cartwright, I., Morgenstern, U., 2016b. Using tritium to document the mean transit time and sources of water contributing to a chain-of-ponds river system: implications for resource protection. *Appl. Geochem.* 75, 9–19. <https://doi.org/10.1016/j.apgeochem.2016.10.007>.
- Cartwright, I., Weaver, T.R., Fifield, L.K., 2006. Cl/Br ratios and environmental isotopes as indicators of recharge variability and groundwater flow: an example from the southeast Murray Basin, Australia. *Chem. Geol.* 231, 38–56. <https://doi.org/10.1016/j.chemgeo.2005.12.009>.
- Cartwright, I., Weaver, T.R., Stone, D., Reid, M., 2007. Constraining modern and historical recharge from bore hydrographs,  $^3\text{H}$ ,  $^{14}\text{C}$ , and chloride concentrations: applications to dual-porosity aquifers in dryland salinity areas, Murray Basin, Australia. *J. Hydrol.* 332, 69–92. <https://doi.org/10.1016/j.jhydrol.2006.06.034>.
- Cook, P.G., Böhlke, J.K., 2000. Determining timescales for groundwater flow and solute transport. In: Cook, P.G., Herczeg, A.L. (Eds.), *Environmental Tracers in Subsurface Hydrology*. Kluwer, Boston, pp. 1–30.
- Crosbie, R., Morrow, D., Cresswell, R., Leaney, F., Lamontagne, S., Lefournour, M., 2012. New insights to the chemical and isotopic composition of rainfall across Australia. CSIRO Water for a Healthy Country Flagship, Australia.
- Department of Environment Land Water and Planning, 2017. State Government Victoria Department of Environment Environment, Land, Water and Planning Water Measurement Information System. <http://data.water.vic.gov.au/monitoring.htm>.
- Diersch, H.J., 2013. FEFLOW: Finite Element Modeling of Flow, Mass and Heat Transport in Porous and Fractured Media. Springer Science & Business Media.
- Duvert, C., Stewart, M.K., Cendón, D.I., Raiber, M., 2016. Time series of tritium, stable isotopes and chloride reveal short-term variations in groundwater contribution to a stream. *Hydrol. Earth Syst. Sci.* 20, 257–277. <https://doi.org/10.5194/hess-20-257-2016>.
- Energy and Earth Resources, 2017. State Government Victoria Department of Economic Development, Jobs, Transport and Resources. <http://www.energyandresources.vic.gov.au/earth-resources/maps-reports-and-data/geovic>.
- Freeman, M.C., Pringle, C.M., Jackson, C.R., 2007. Hydrologic connectivity and the contribution of stream headwaters to ecological integrity at regional scales. *J. Am. Water Resour. Assoc.* 43, 5–14. <https://doi.org/10.1111/j.1752-1688.2007.00002.x>.
- Godsey, S.E., Kirchner, J.W., Clow, D.W., 2009. Concentration-discharge relationships reflect chemostatic characteristics of US catchments. *Hydrol. Process.* 23, 1844–1864. <https://doi.org/10.1002/hyp.7315>.
- Herczeg, A.L., Dogramaci, S.S., Leaney, F.W., 2001. Origin of dissolved salts in a large, semi-arid groundwater system: Murray Basin, Australia. *Mar. Freshwater Res.* 52, 41–52. <https://doi.org/10.1071/MF00040>.
- Howcroft, W., Cartwright, I., Morgenstern, U., 2017. Mean transit times in headwater catchments: insights from the Otway Ranges, Australia. *Hydrol. Earth Syst. Sci.* <https://doi.org/10.5194/hess-2017-219>.
- Hrachowitz, M., Savenije, H., Bogaard, T.A., Tetzlaff, D., Soulsby, C., 2013. What can flux tracking teach us about water age distribution patterns and their temporal dynamics? *Hydrol. Earth Syst. Sci.* 17, 533–564. <https://doi.org/10.5194/hess-17-533-2013>.
- Hrachowitz, M., Soulsby, C., Tetzlaff, D., Dawson, J.J.C., Dunn, S.M., Malcolm, I.A., 2009a. Using long-term data sets to understand transit times in contrasting headwater catchments. *J. Hydrol.* 367, 237–248. <https://doi.org/10.1016/j.jhydrol.2009.01.001>.
- Hrachowitz, M., Soulsby, C., Tetzlaff, D., Dawson, J.J.C., Malcolm, I.A., 2009b. Regionalization of transit time estimates in montane catchments by integrating landscape controls. *Water Resour. Res.* 45, W05421. <https://doi.org/10.1029/2008WR007496>.
- Hrachowitz, M., Soulsby, C., Tetzlaff, D., Speed, M., 2010. Catchment transit times and landscape controls—Does scale matter? *Hydrol. Process.* 24, 117–125. <https://doi.org/10.1002/hyp.7510>.
- International Atomic Energy Agency, 2017. Global Network of Isotopes in Precipitation. <http://www.iaea.org/water>.
- Jurgens, B.C., Böhlke, J.K., Eberts, S.M., 2012. TracerLPM (Version 1): An Excel® workbook for interpreting groundwater age distributions from environmental tracer data. U.S. Geological Survey Techniques and Methods Report 4-F3, p.60.
- Kirchner, J.W., 2016. Aggregation in environmental systems—Part 1: seasonal tracer cycles quantify young water fractions, but not mean transit times, in spatially heterogeneous catchments. *Hydrol. Earth Syst. Sci.* 20, 279–297. <https://doi.org/10.5194/hess-20-279-2016>.
- Lachassagne, P., Wyns, R., Dewandel, B., 2011. The fracture permeability of hard rock aquifers is due neither to tectonics, nor to unloading, but to weathering processes. *Terra Nova* 23, 145–161. <https://doi.org/10.1111/j.1365-3121.2011.00998.x>.
- Leray, S., Engdahl, N.B., Massoudieh, A., Bresciani, E., McCallum, J., 2016. Residence time distributions for hydrologic systems: mechanistic foundations and steady-state analytical solutions. *J. Hydrol.* 543, 67–87. <https://doi.org/10.1016/j.jhydrol.2016.01.068>.
- Maloszewski, P., 2000. Lumped-parameter models as a tool for determining the hydrological parameters of some groundwater systems based on isotope data. *IAHS-AISH Publ.* 262, 271–276.
- Maloszewski, P., Zuber, A., 1982. Determining the turnover time of groundwater systems with the aid of environmental tracers: 1. Models and their applicability. *J. Hydrol.* 57, 207–231. [https://doi.org/10.1016/0022-1694\(82\)90147-0](https://doi.org/10.1016/0022-1694(82)90147-0).
- Melbourne Water, 2014. Woori Yallock water supply protection area stream flow annual report. [www.melbournwater.com.au](http://www.melbournwater.com.au).
- Melbourne Water, 2017. Rainfall and river level data. <https://www.melbournwater.com.au/water/rainfall-and-river-levels/#/>.
- McCallum, J.L., Cook, P.G., Simmons, C.T., 2015. Limitations of the use of environmental tracers to infer groundwater age. *Groundwater* 53, 56–70. <https://doi.org/10.1111/gwat.12237>.
- McCallum, J.L., Cook, P.G., Simmons, C.T., Werner, A.D., 2014. Bias of apparent tracer ages in heterogeneous environments. *Groundwater* 52, 239–250. <https://doi.org/10.1111/gwat.12052>.
- McDonnell, J.J., McGuire, K., Aggarwal, P., Beven, K.J., Biondi, D., Destouni, G., Dunn, S., James, A., Kirchner, J., Kraft, P., Lyon, S., Maloszewski, P., Newman, B., Pfister, L., Rinaldo, A., Rodhe, A., Sayama, T., Seibert, J., Solomon, K., Soulsby, C., Stewart, M., Tetzlaff, D., Tobin, C., Troch, P., Weiler, M., Western, A., Wörmann, A., Wrede, S., 2010. How old is streamwater? Open questions in catchment transit time

- conceptualization, modelling and analysis. *Hydrol. Process.* 24, 1745–1754. <https://doi.org/10.1002/hyp.7796>.
- McGuire, K.J., McDonnell, J.J., 2006. A review and evaluation of catchment transit time modeling. *J. Hydrol.* 330, 543–563. <https://doi.org/10.1016/j.jhydrol.2006.04.020>.
- McGuire, K.J., McDonnell, J.J., Weiler, M., Kendall, C., McGlynn, B.L., Welker, J.M., Seibert, J., 2005. The role of topography on catchment-scale water residence time. *Water Resour. Res.* 41, 1–14. <https://doi.org/10.1029/2004WR003657>.
- Morgenstern, U., Daughney, C.J., Leonard, G., Gordon, D., Donath, F.M., Reeves, R., 2015. Using groundwater age and hydrochemistry to understand sources and dynamics of nutrient contamination through the catchment into Lake Rotorua, New Zealand. *Hydrol. Earth Syst. Sci.* 19, 803–822. <https://doi.org/10.5194/hess-19-803-2015>.
- Morgenstern, U., Stewart, M.K., Stenger, R., 2010. Dating of streamwater using tritium in a post nuclear bomb pulse world: continuous variation of mean transit time with streamflow. *Hydrol. Earth Syst. Sci.* 14, 2289–2301. <https://doi.org/10.5194/hess-14-2289-2010>.
- Morgenstern, U., Taylor, C.B., 2009. Ultra low-level tritium measurement using electrolytic enrichment and LSC. *Isot. Environ. Health Stud.* 45, 96–117. <https://doi.org/10.1080/10256010902931194>.
- Rice, K.C., Hornberger, G.M., 1998. Comparison of hydrochemical tracers to estimate source contributions to peak flow in a small, forested, headwater catchment. *Water Resour. Res.* 34, 1755–1766. <https://doi.org/10.1029/98WR00917>.
- Shugg, A., 1996. *Hydrogeology of the Dandenong Ranges Fractured Rock Aquifers and the Comparison with Similar Aquifers in Victoria* MSc Thesis. Sydney University of Technology, Sydney, Australia.
- Soulsby, C., Birkel, C., Geris, J., Tetzlaff, D., 2015. Spatial aggregation of time-variant stream water ages in urbanizing catchments. *Hydrol. Process.* 29, 3038–3050. <https://doi.org/10.1002/hyp.10500>.
- Soulsby, C., Malcolm, I.A., Youngson, A.F., Tetzlaff, D., Gibbins, C.N., Hannah, D.M., 2005. Groundwater-surface water interactions in upland Scottish rivers; hydrological, hydrochemical and ecological implications. *Scott. J. Geol.* 41, 39–49. <https://doi.org/10.1144/sjg41010039>.
- Soulsby, C., Tetzlaff, D., Hrachowitz, M., 2009. Tracers and transit times: windows for viewing catchment scale storage? *Hydrol. Process.* 23, 3503–3507. <https://doi.org/10.1002/hyp.7501>.
- Southern Rural Water, 2014. Latrobe River Basin. [www.srw.com.au](http://www.srw.com.au).
- Speed, M., Tetzlaff, D., Soulsby, C., Hrachowitz, M., Waldron, S., 2010. Isotopic and geochemical tracers reveal similarities in transit times in contrasting mesoscale catchments. *Hydrol. Process.* 24, 1211–1224. <https://doi.org/10.1002/hyp.7593>.
- Stewart, M.K., Morgenstern, U., Gusyev, M.A., Maloszewski, P., 2017. Aggregation effects on tritium-based mean transit times and young water fractions in spatially heterogeneous catchments and groundwater systems. *Hydrol. Earth Syst. Sci.* 21, 4615–4627. <https://doi.org/10.5194/hess-21-4615-2017>.
- Stewart, M.K., Morgenstern, U., McDonnell, J.J., 2010. Truncation of stream residence time: how the use of stable isotopes has skewed our concept of streamwater age and origin. *Hydrol. Process.* 24, 1646–1659. <https://doi.org/10.1002/hyp.7576>.
- Stewart, M.K., Morgenstern, U., McDonnell, J.J., Pfister, L., 2012. The 'hidden streamflow' challenge in catchment hydrology: a call to action for stream water transit time analysis. *Hydrol. Process.* 26, 2061–2066. <https://doi.org/10.1002/hyp.9262>.
- Stewart, M.K., Stevens, G., Thomas, J.T., van der Raaij, R., Trompeter, V., 2011. Nitrate sources and residence times of groundwater in the Waimea Plains, Nelson. *J. Hydrol. N.Z.* 50, 313–338.
- Suckow, A., 2014. The age of groundwater – definitions, models and why we do not need this term. *Appl. Geochem.* 50, 222–230. <https://doi.org/10.1016/j.apgeochem.2014.04.016>.
- Tadros, C.V., Hughes, C.E., Crawford, J., Hollins, S.E., Chisari, R., 2014. Tritium in Australian precipitation: a 50 year record. *J. Hydrol.* 513, 262–273. <https://doi.org/10.1016/j.jhydrol.2014.03.031>.
- Tetzlaff, D., Soulsby, C., 2008. Sources of baseflow in larger catchments – using tracers to develop a holistic understanding of runoff generation. *J. Hydrol.* 359, 287–302. <https://doi.org/10.1016/j.jhydrol.2008.07.008>.
- Tweed, S.O., Weaver, T.R., Cartwright, I., 2005. Distinguishing groundwater flow paths in different fractured-rock aquifers using groundwater chemistry: Dandenong Ranges, southeast Australia. *Hydrogeol. J.* 13, 771–786. <https://doi.org/10.1007/s10040-004-0348-y>.
- van den Berg, A.H.M., 1975. Definitions and descriptions of Middle Ordovician to Middle Devonian rock units of the Warburton district, east central Victoria. Geological Survey of Victoria. Report, 1975/6.
- van den Berg, A.H.M., Morand, V., 1997. Wangaratta. Geological Society of Victoria 1:250,000 Geological Map Series, Melbourne, Australia, 1997.
- Victoria Open Data, 2016. Victorian Government Data Directory. <https://www.data.vic.gov.au/>.
- Weissmann, G.S., Zhang, Y., LaBolle, E.M., Fogg, G.E., 2002. Dispersion of groundwater age in an alluvial aquifer system. *Water Resour. Res.* 38, 1198. <https://doi.org/10.1029/2001WR000907>.
- Winter, T.C., 1999. Relation of streams, lakes, and wetlands to groundwater flow systems. *Hydrogeol. J.* 7, 28–45. <https://doi.org/10.1007/s100400050178>.